

# Coherence-assisted single-shot cooling by quantum absorption refrigerators

Mark T. Mitchison,<sup>1</sup> Mischa P. Woods,<sup>2,3</sup> Javier Prior,<sup>4</sup> and Marcus Huber<sup>5,6</sup>

<sup>1</sup>*Quantum Optics and Laser Science Group, Blackett Laboratory,  
Imperial College London, London SW7 2BW, United Kingdom*

<sup>2</sup>*Centre for Quantum Technologies, National University of Singapore, 3 Science Drive 2, Singapore 117543*

<sup>3</sup>*University College of London, Department of Physics & Astronomy, London WC1E 6BT, United Kingdom*

<sup>4</sup>*Universidad Politécnica de Cartagena, C/Dr Fleming S/N 30202 Cartagena, Spain*

<sup>5</sup>*Departament de Física, Universitat Autònoma de Barcelona, E-08193 Bellaterra, Spain*

<sup>6</sup>*ICFO-Institut de Ciències Fotoniques, Mediterranean Technology Park, 08860 Castelldefels (Barcelona), Spain*

(Dated: December 3, 2024)

The extension of thermodynamics into the quantum regime has received much attention in recent years. A primary objective of current research is to find thermodynamic tasks which can be enhanced by quantum mechanical effects. With this goal in mind, we explore the finite-time dynamics of absorption refrigerators composed of three qubits. The aim of this finite-time cooling is to reach low temperatures as fast as possible and subsequently extract the cold particle to exploit it for information processing purposes. We show that the coherent oscillations inherent to quantum dynamics can be harnessed to reach temperatures that are colder than the steady state in orders of magnitude less time, thereby providing a fast source of low-entropy qubits. This effect demonstrates that quantum thermal machines can surpass classical ones, reminiscent of quantum advantages in other fields, and is applicable to a broad range of technologically important scenarios.

## INTRODUCTION

The development of classical thermodynamics in the 19th century underpinned the Industrial Revolution, and the enormous economic growth and social changes that followed. Now, in the 21st century, the burgeoning quantum technological revolution promises unprecedented advances in our computation and communication capabilities, enabled by harnessing quantum coherence. As our machines are scaled down into the quantum regime, it is of prime importance to understand how quantum mechanics affects the operation of these devices. This problem has attracted great interest to the field of quantum thermodynamics over the last few years.

One useful approach in this regard is to explore simple physical models which highlight novel aspects of quantum thermal machines. The quantum absorption refrigerator is the quantum extension of a classical machine devised in the 19th century (see for example Ref. [1] and references therein). The smallest possible model with couplings between physical particles and thermal reservoirs was first studied by Linden et al. [2]. While the history of studying these machines dates back a long time even in the quantum regime, the three-qubit model was the first where the role of quantum information resources was studied [3], revealing that entanglement in the steady state prohibits achieving perfect Carnot efficiency, but potentially increases cooling efficiency.

Designing thermodynamic processes that can be enhanced by quantum dynamics is a pivotal challenge in the field of quantum thermodynamics. One of the paradigmatic thermodynamic tasks concerns work efficiency at the quantum scale. Here already the very definition of quantum mechanical work is debated [4–6], yet in dif-

ferent scenarios quantum mechanical advantages seem possible [7–9]. Another avenue in this endeavour is the engineering of the environment itself to enhance quantum processes [10–13]. We circumvent the potential controversies regarding the practical value of work and efficiency by concentrating on a different figure of merit and by using thermal baths to drive the refrigerator, therefore needing no notion of work.

Previous work on the quantum aspects of heat engines and refrigerators has focused almost exclusively on their operation in the steady state. However, in many applications one wishes to reach low temperatures as rapidly as possible, in which case understanding the short-time behaviour is essential. In particular, the cooling may be applied only transiently, after which the cold object is extracted for use. As a somewhat frivolous yet illustrative example, consider the problem of refrigerating a freshly bought bottle of beer on a hot day. Maximum enjoyment is obtained if the beer can be consumed quickly, and at a temperature significantly lower than that of the environment. A more serious example could be the initialisation of a register of qubits for quantum information processing, where the aim is to produce states with high purity (low entropy). Fast cooling is advantageous here since it may reduce the overall time taken to complete the quantum information protocol. Both of these situations exemplify what we call *single-shot cooling*: the one-time application of a refrigeration device in order to considerably and rapidly reduce the temperature of the object in question.

In the present work, we study the application of three-qubit absorption refrigerators to single-shot cooling. By considering variations of the basic processes underlying energy dissipation and transport, we elucidate the role of coherence in the operation of such a device. Further-

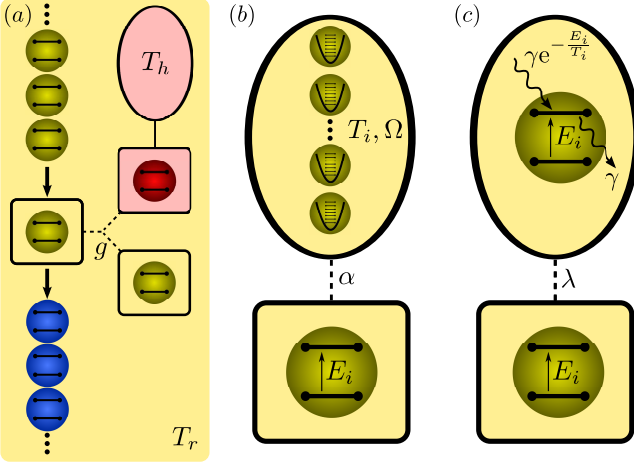


FIG. 1. Cartoon illustrating our theoretical set-up. (a) A stream of thermal qubits passes sequentially through a quantum absorption refrigerator. Each thermal qubit interacts with the refrigerator for a finite time, and exits the device at a lower temperature. (b) We model Markovian reservoirs as an infinite collection of harmonic oscillators, characterised by a bandwidth  $\Omega$  and a dimensionless coupling strength  $\alpha$ . (c) We model narrow-band reservoirs by a single fictitious qubit undergoing Markovian gain and decay processes, characterised by a linewidth  $\gamma$  and a coupling energy  $\lambda$ .

more, we demonstrate that dramatic improvements can be obtained in both the cooling time and the achievable temperatures by taking advantage of coherent oscillations that appear in the transient dynamics of the refrigerator. Note that a physical implementation of a quantum heat engine has recently been proposed in a trapped-ion set-up [14]. Our findings could thus be applicable to current and near-future experiments, which may be practically limited by finite coherence times. From a more fundamental perspective, our scheme provides one of the first examples in which quantum coherence plays an active and necessary role in improving the performance of thermal machines.

## THEORETICAL FRAMEWORK

### Description of the Refrigerator

The quantum absorption refrigerator comprises three qubits described by standard Pauli operators  $\sigma_i^{x,y,z}$ , with the local Hamiltonian

$$H_{\text{loc}} = \frac{1}{2} \sum_{i=1}^3 E_i (\mathbb{1} + \sigma_i^z). \quad (1)$$

Throughout this article, we employ units of energy, time and temperature such that  $E_1 = 1$ ,  $\hbar = 1$  and  $k_B = 1$ . The qubits are coupled together according to a three-

body interaction

$$H_{\text{int}} = g |010\rangle\langle101| + \text{h.c.}, \quad (2)$$

where the computational basis states  $|0\rangle$ ,  $|1\rangle$  denote the eigenvectors of  $\sigma^z$ . In order for this interaction to be energy-conserving, in the sense that  $[H_{\text{loc}}, H_{\text{int}}] = 0$ , we demand that the qubit energies satisfy  $E_2 = E_1 + E_3$ . The interaction (2) then drives resonant transitions within the *transport subspace* spanned by the states  $|010\rangle$  and  $|101\rangle$ .

Each qubit  $i$  is in contact with an independent heat bath  $B_i$ , which drives it towards a thermal equilibrium state at inverse temperature  $\beta_i = 1/T_i$ , where  $T_1 \leq T_2 < T_3$ . When the system parameters are judiciously chosen, the dynamics propels qubit 1 (the ‘‘cold qubit’’) towards a new temperature  $\tilde{T}_1 < T_1$ . It is in this sense that the system behaves as a refrigerator, whose basic operating principle may be understood as follows. The interaction Hamiltonian (2) couples the cold qubit to a ‘‘virtual qubit’’ [15] comprising the  $\{|01\rangle, |10\rangle\}$  subspace of the Hilbert space of qubits 2 and 3. When these qubits are at equilibrium with their respective baths, the populations of the virtual qubit states are thermally distributed at an effective temperature given by

$$T_{\text{eff}} = \frac{E_2 - E_3}{\beta_2 E_2 - \beta_3 E_3}. \quad (3)$$

If the parameters of the refrigerator are arranged so that  $T_{\text{eff}} < T_1$ , then the cold qubit equilibrates to a lower temperature as it exchanges energy with the virtual qubit on the approach to the steady state.

In the following, we specialise to the case where  $T_1 = T_2 =: T_r$ , and we define  $T_h := T_3$ . This is in many ways the most natural scenario, where we have a single source of free energy — namely the hot bath at temperature  $T_h$  — enabling us to cool below the ambient ‘‘room temperature’’  $T_r$ . So long as qubits 1 and 2 are sufficiently spatially separated<sup>1</sup>, we can treat the effect of their common environment as arising from two independent baths [16].

The general set-up that we have in mind is illustrated in Fig. 1(a). We assume that all three qubits are initially in thermal equilibrium with their respective reservoirs. At time  $t = 0$  the interaction (2) between the qubits is switched on. The aim is then to *prepare* the cold qubit in a low-entropy state. (We emphasise that this is quite different from the usual objective considered by previous authors, namely to *maintain* the cold qubit at a low temperature.) Once the lowest achievable temperature has been reached, our cooling protocol is complete, and

<sup>1</sup> More precisely, the distance between the two qubits must be much greater than the correlation length  $\xi = c/\Omega$ , where  $c$  is a characteristic velocity of bath excitations and  $\Omega$  is the frequency cut-off characterising the bandwidth of environmental noise.

the cold qubit may be extracted for use, for example, in quantum information processing. If we suppose now that there exists a large supply of qubits thermalised to the ambient temperature  $T_r$ , we can perform this protocol repeatedly to produce a steady stream of low-entropy qubits.

### Models of Thermalisation

In order to quantitatively analyse the refrigerator we must specify a thermalisation model. On the other hand, one would like to obtain general results that are independent of any particular model. In order to avoid being too restricted by our assumptions, we employ three different approaches to modelling the thermalising effect of the heat baths, each valid in a different parameter regime. In the following paragraphs, we describe these models in a qualitative way, deferring the full details to the Appendix.

A common assumption of statistical mechanics is that the baths are Markovian (memory-less). To model this scenario, we suppose that each qubit is coupled to an infinite collection of harmonic oscillators spanning a broad range of frequencies (Fig. 1(b)). The baths are described by identical Ohmic spectral functions of the form

$$J(\omega) = \alpha \omega e^{-\omega/\Omega}. \quad (4)$$

This function quantifies the strength of the coupling between each qubit and the oscillators near frequency  $\omega$ , weighted by the density of states of the reservoir (see Appendix). The effect of the baths is therefore characterised by two parameters: a dimensionless coupling strength  $\alpha$ , and a frequency cut-off  $\Omega$  leading to a bath memory time of order  $\Omega^{-1}$ . Markovian dynamics is obtained when  $\Omega$  is much larger than all other frequency scales and  $\alpha \ll 1$ , so that the dissipation rates are much smaller than the natural frequencies  $\{E_i\}$  of the qubits. Some care must be taken when treating the effect of the inter-qubit coupling on the thermalisation dynamics. We are able to derive two different master equations depending on the magnitude of  $g$ . The first equation is valid in the strong-coupling limit, where  $g$  is much larger than the dissipation rates [17]. The second master equation holds in the weak-coupling limit, when  $g$  is comparable to or smaller than the dissipation rates [18, 19].

If each qubit only couples to a narrow range of frequencies in the reservoirs, bath memory effects may be significant and the Markov assumption is invalid. We model this situation by assigning to each qubit of the refrigerator an additional fictitious qubit, and allowing excitations to hop between the two qubits at a rate  $\lambda$ . Each fictitious qubit is then connected to a perfectly Markovian thermal bath, such that the spontaneous emission rate is  $\gamma$  (Fig. 1(c)), thus simulating an effective non-Markovian

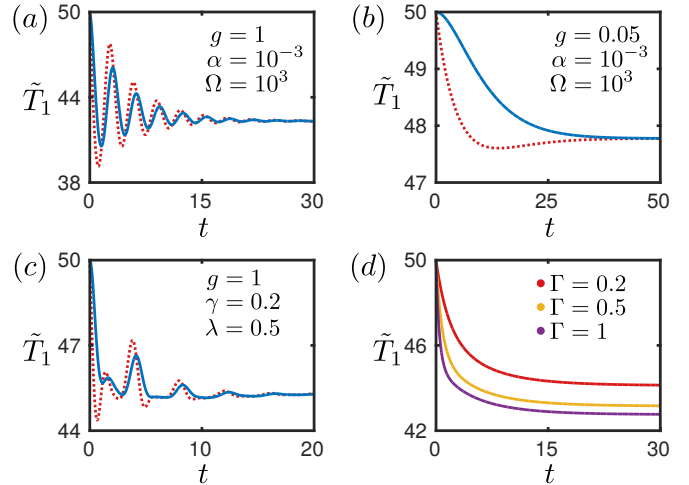


FIG. 2. Typical examples of the effective temperature dynamics of the cold qubit according to four different models of a quantum absorption refrigerator: (a) strong-coupling Markovian master equation, (b) weak-coupling Markovian master equation, (c) the fictitious bath-qubit model and (d) the stochastic transport model for three different qubit-qubit couplings and with the same bath parameters as (a). Blue solid lines depict the evolution of an initial thermal product state, red dashed lines show the dynamics when 0.5% of the maximum coherence has been added to the initial state. The other parameters are  $E_2 = 2$ ,  $T_r = 50$  and  $T_h = 100$ .

reservoir with a memory time of order  $\gamma^{-1}$  coupled to the physical qubit. This phenomenological model captures the transition from Markovian to non-Markovian dynamics in a simple way as  $\gamma$  is decreased.

## RESULTS

### Short-Time Dynamics of the Refrigerator

We now present our quantitative results, obtained by numerical solution of the equations of motion. Our first observation is that sufficiently strong coherent coupling between the qubits drives damped Rabi oscillations of the local qubit populations. However, unlike Rabi oscillations due to local driving fields, the three-body interaction (2) does not induce any local coherences between the qubit populations. The reduced state of each qubit is diagonal at all times and may therefore be assigned an effective temperature

$$\tilde{T}_i(t) = \frac{-E_i}{2 \tanh^{-1} \langle \sigma_i^z(t) \rangle}. \quad (5)$$

To illustrate this feature of the short-time dynamics, we plot several examples of the evolution of the cold qubit temperature in Fig. 2, which demonstrate that the Rabi oscillations allow the cold qubit to reach lower temperatures than the steady state. In the strong-coupling

regime under Markovian dissipation, we find damped temperature oscillations with the approximate period  $\pi/g$  (solid line in Fig. 2(a)). Therefore, the optimal single-shot cooling procedure consists of extracting the cold qubit after a time  $t_0 \approx \pi/(2g)$ . A more complicated oscillatory behaviour is possible outside of the Markovian regime, due to the large amounts of coherence between the refrigerator and the baths (solid line in Fig. 2(c)). Nevertheless, a temperature minimum can still occur after a finite time, although the optimum extraction time may be later than  $\pi/(2g)$ . In contrast, when the coupling  $g$  is much smaller than the relaxation rate, these oscillations are over-damped so that no temperature minimum occurs in a finite time (solid line in Fig. 2(b)). In general however, we have found that optimal single-shot cooling in finite time is possible over a very broad range of parameters, so long as the coupling  $g$  is significantly larger than the relaxation rate, and the qubit-bath coupling is sufficiently weak.

The physical origin of these temperature oscillations is the exchange of energy between the refrigerator qubits due to the interaction (2). Our second important observation is that this energy transport is driven by coherence in the transport subspace. This can be seen straightforwardly by examining the Heisenberg equations of motion for the local energy expectation values  $h_i = E_i \langle \sigma_i^z \rangle / 2$ . The resulting expression for the cold qubit is of the form

$$\frac{dh_1}{dt} = \dot{Q}_1(t) + 2gE_1\mathcal{C}(t). \quad (6)$$

This equation represents an energy balance between the rate of heat absorbed by the bath  $\dot{Q}_1(t)$  and the coherent flow of energy into the other qubits, which is proportional to the imaginary part of the coherence in the transport subspace:

$$\mathcal{C}(t) = \text{Im} \text{ Tr} [\rho(t)|101\rangle\langle 010|], \quad (7)$$

where  $\rho(t)$  denotes the quantum state. Eqs. (6) & (7) give a direct link between the presence of coherence in the transport subspace and the flow of energy across the refrigerator.

To further elucidate the fundamental role of coherence in energy transport, we consider a situation where some initial coherence in the transport subspace is added to the initial state, without modifying the thermally distributed populations. In order to ensure the positivity of the quantum state, this coherence is upper bounded by

$$\mathcal{C}_{\max} = \prod_{i=1}^3 \frac{1}{2} \text{sech} \left( \frac{\beta_i E_i}{2} \right). \quad (8)$$

For each example in Figs. 2(a-c) we have also plotted the dynamics with a very small amount of initial coherence  $\mathcal{C}(0) = 0.005\mathcal{C}_{\max}$  added. We find that the amplitude of the temperature oscillations is noticeably enhanced

in all three cases. In the weak-coupling example plotted (dashed line in Fig. 2(b)), the initial coherence gives the most dramatic advantage, since now the temperature minimum occurs in finite time. Initial coherence is actually a necessary ingredient for single-shot cooling in this case and thus should be considered as an additional non-classical resource to the free energy of the hot bath. In the non-Markovian evolution plotted in Fig. 2(c), the addition of coherence shifts the temperature minimum forward to approximately  $t_0 \approx \pi/(2g)$ , which could be a useful effect when fast operation of the single-shot cooling protocol is a priority.

Note that according to Eq. (6) the sign of  $\mathcal{C}(0)$  determines the direction of the initial flow of energy into the qubit. Therefore, it is even possible, for example, to heat the qubit by adding initial coherence with the opposite sign, even when the system behaves as a refrigerator in the steady state. Likewise one can transiently cool even when the steady-state behaviour is that of a heat pump. Similar phase effects have recently been described in Ref. [20] where the authors study the effect that a physical environment can exert on the early time evolution of certain initial superposition states of open quantum systems. Depending on the system phase, bath fluctuations can revert the detailed balance condition, creating a net flux of energy from the environment into the system.

Overall, we have found strong evidence that coherence is a useful resource that may be harnessed to produce a significant advantage to single-shot cooling. Conversely, we can show that no advantage is obtained in the absence of coherence. In particular, we consider a stochastic three-qubit absorption refrigerator model where the qubits exchange energy only incoherently (details in the Appendix). The system still works as a refrigerator, since the steady-state temperature of the cold qubit may be lower than  $T_1$ . However, the relaxation dynamics exhibits pure exponential decay, as depicted for some examples in Fig. 2(d). Therefore, no temperature minimum occurs in finite time, precluding the possibility of single-shot cooling below the steady-state temperature.

### Quantum Coherent Advantage Time

As we have shown, coherence in the quantum absorption refrigerator allows us to transiently cool below the steady-state temperature. However, once the cold qubit is decoupled from the refrigerator at time  $t_0$ , its temperature begins to increase as it equilibrates with the room-temperature bath. Therefore, the advantage gained from transient cooling only lasts until the cold qubit's temperature grows larger than the steady state temperature, which occurs at a time  $t_1$ . This motivates us to define the quantum advantage time  $t_Q = t_1 - t_0$ , which quantifies the time elapsed after the single-shot cooling

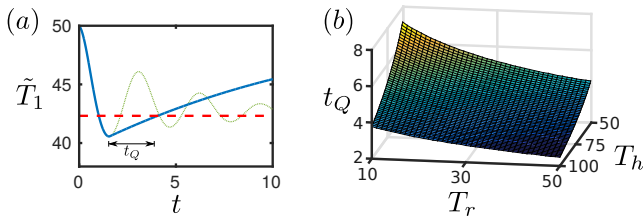


FIG. 3. (a) The quantum advantage time  $t_Q$  is defined as the time elapsed between the switch-off of the cooling protocol and the point when the temperature of the cold qubit (solid blue line) reaches that of the steady-state (dashed red line). The same parameters as Fig. 2(a) are used, with the full evolution without a switch-off shown by the dotted green line. (b) The advantage time as a function of the ambient and hot bath temperatures, with  $g = 1$ .

during which the quantum coherent advantage persists (Fig. 3(a)).

For simplicity, in this section we work in the Markovian strong-coupling limit, where there always exists some single-shot cooling advantage and the switch-off time is given approximately by  $t_0 \approx \pi/(2g)$  in all cases. We have found numerically that for fixed couplings  $g$ ,  $\alpha$  and  $\Omega$ , the quantum advantage time  $t_Q$  is independent of  $E_2$ , and therefore is a function only of the bath temperatures. This dependence is plotted for an example in Fig. 3(b). We find that the quantum advantage persists for longest when both the ambient and hot bath temperatures are low.

## CONCLUSIONS

We have studied the dynamical evolution of three qubit refrigerators in different regimes, using three different standard models of dissipation in open quantum systems. In all of these we encounter oscillations in the temperature of the target qubit below the equilibrium temperature, reinforcing the notion of a universal and robust feature of quantum refrigerators. Since the initial states we consider come for free in the context of thermodynamic resource theories [21], or more explicitly come directly from their respective baths, we show that with the right timing these oscillations can be exploited to yield a constant stream of cold qubits. Numerous quantum information processing protocols require (approximately) pure input states [22], potentially making quantum thermal machines a useful addition as pre-cursors to information processing protocols. The advantage of the quantum absorption refrigerator lies in its high degree of autonomy: no external energy source is required to keep the machine running, and control is required only over the qubit-qubit interaction. Two thermal baths at a given temperature are sufficient to let the machines run for as long as their temperatures do not change significantly

(which for macroscopic baths in contact with quantum systems is sufficiently long for all practical purposes).

Apart from the prospect of information processing these results help elucidate the quantum nature of thermodynamics. Compared to classical thermodynamics its counterpart at the quantum scale often results in additional constraints and limitations [5, 23] due to the discretised nature of the fundamental states. The central question in this context concerns the actual impact of coherence, entanglement and other genuine quantum features on the potential transformations in quantum thermodynamics. Indeed researchers have only just recently started investigating coherences in the context of resource theories, and a complete understanding is still elusive [24]. As we show using the stochastic absorption refrigerator, even three-particle fridges are in some sense equivalent to classical ones, as one can reach similar results in the steady state. On the other hand, the coherent transport of energy inducing oscillations in the population of the cold qubits constitutes a unique quantum feature. This points towards the potential of harnessing genuine quantum resources to take thermal machines beyond the classically possible.

## ACKNOWLEDGEMENTS

We acknowledge inspiring discussions with Jonathan Bohr-Brask, Nicolas Brunner, Karen Hovhannisyan, Marti Perarnau and Martin Plenio. We also thank Martin Plenio for helpful comments on the manuscript. M.T.M. acknowledges financial support from the UK EPSRC. M.W. acknowledges funding from the Singaporean ministry of education, Tier 3 Grant Random numbers from quantum processes (MOE2012-T3-1-009). J.P. acknowledges funding by the Spanish Ministerio de Economía y Competitividad under Project No. FIS2012-30625. M.H. acknowledges funding from the Juan de la Cierva fellowship (JCI 2012-14155), the European Commission (STREP "RAQUEL") and the Spanish MINECO Project No. FIS2013-40627-P, the Generalitat de Catalunya CIRIT Project No. 2014 SGR 966.

---

- [1] A. Levy and R. Kosloff. The quantum absorption refrigerator. arXiv:1109.0728 [quant-ph], 2011.
- [2] N. Linden, S. Popescu, and P. Skrzypczyk. How small can thermal machines be? The smallest possible refrigerator. *Phys. Rev. Lett.*, 105:130401, 2010.
- [3] N. Brunner, M. Huber, N. Linden, S. Popescu, R. Silva, and P. Skrzypczyk. Entanglement enhances cooling in microscopic quantum refrigerators. *Phys. Rev. E*, 89(3):32115, 2014.
- [4] A. E. Allahverdyan, R. S. Johal, and G. Mahler. Work extremum principle: Structure and function of quantum heat engines. *Phys. Rev. E*, 77(4):041118, 2008.

[5] M. Horodecki and J. Oppenheim. Fundamental limitations for quantum and nanoscale thermodynamics. *Nat. Comm.*, 4:2059, 2013.

[6] P. Skrzypczyk, A. J. Short, and S. Popescu. Work extraction and thermodynamics for individual quantum systems. *Nat. Comm.*, 5:4185, 2014.

[7] S. De Liberato and M. Ueda. Carnot's theorem for nonthermal stationary reservoirs. *Phys. Rev. E*, 84(5):051122, 2011.

[8] M. Perarnau-Llobet, K. V. Hovhannisyan, M. Huber, P. Skrzypczyk, N. Brunner, and A. Acín. Extracting work from correlations. arXiv:1407.7765 [quant-ph], 2014.

[9] K. Brandner, M. Bauer, M. T. Schmid, and U. Seifert. Coherence-enhanced efficiency of feedback-driven quantum engines. page 14, 2015. arXiv:1503.04865 [quant-ph].

[10] L. A. Correa, J. P. Palao, D. Alonso, and G. Adesso. Quantum-enhanced absorption refrigerators. *Sci. Rep.*, 4, 2014.

[11] J. Roßnagel, O. Abah, F. Schmidt-Kaler, K. Singer, and E. Lutz. Nanoscale heat engine beyond the carnot limit. *Phys. Rev. Lett.*, 112:030602, 2014.

[12] N. Killoran, S. F. Huelga, and M. B. Plenio. Enhancing light-harvesting power with coherent vibrational interactions: a quantum heat engine picture. arXiv:1412.4136 [physics.chem-ph], 2014.

[13] J. Lim, D. Paleček, F. Caycedo-Soler, C. N. Lincoln, J. Prior, H. von Berlepsch, S. F. Huelga, M. B. Plenio, D. Zigmantas, and J. Hauer. Verification of the vibronic origin of long-lived coherence in an artificial molecular light harvester. arXiv:1502.01717 [physics.chem-ph], 2015.

[14] O. Abah, J. Roßnagel, G. Jacob, S. Deffner, F. Schmidt-Kaler, K. Singer, and E. Lutz. Single-ion heat engine at maximum power. *Phys. Rev. Lett.*, 109:203006, 2012.

[15] N. Brunner, N. Linden, S. Popescu, and P. Skrzypczyk. Virtual qubits, virtual temperatures, and the foundations of thermodynamics. *Phys. Rev. E*, 85:051117, 2012.

[16] G. M. Palma, K.-A. Suominen, and A. K. Ekert. Quantum computers and dissipation. *Proc. Roy. Soc. A*, 452(1946):567–584, 1996.

[17] L. A. Correa, J. P. Palao, G. Adesso, and D. Alonso. Performance bound for quantum absorption refrigerators. *Phys. Rev. E*, 87:042131, 2013.

[18] H. Wichterich, M. J. Henrich, H. Breuer, J. Gemmer, and M. Michel. Modeling heat transport through completely positive maps. *Phys. Rev. E*, 76:031115, 2007.

[19] Á. Rivas, A. D. K. Plato, S. F. Huelga, and M. B. Plenio. Markovian master equations: a critical study. *New J. Phys.*, 12(11):113032, 2010.

[20] S. Oviedo, J. Prior, R. Rosenbach, A. Chin, S. F. Huelga, and M. B. Plenio. Phase-dependent exciton transport and non-equilibrium energy harvesting from thermal environments. In preparation.

[21] M. Horodecki and J. Oppenheim. (Quantumness in the context of) resource theories. *Int. J. Mod. Phys. B*, (27):1345019, 2013.

[22] M. L. Nielsen and I. L. Chuang. *Quantum Computation and Quantum Information*. Cambridge University Press, 2000.

[23] F. G. S. L. Brandão, M. Horodecki, N. H. Y. Ng, J. Oppenheim, and S. Wehner. The second laws of quantum thermodynamics. *Proc. Nat. Ac. Sci.*, 112(11):201411728, 2015.

[24] M. Lostaglio, D. Jennings, and T. Rudolph. Description of quantum coherence in thermodynamic processes requires constraints beyond free energy. *Nat. Comm.*, 6:6383, 2015.

[25] H. P. Breuer and F. Petruccione. *The Theory of Open Quantum Systems*. Oxford University Press, 1st edition, 2007.

## APPENDIX

### Strong-Coupling Master Equation

In this section we derive the Markovian master equation in the strong-coupling limit, following Correa et al. [17]. We model each heat bath as a collection of harmonic oscillators, so that the total Hamiltonian for the three baths is  $H_B = \sum_{i=1}^3 H_{B_i}$ , with

$$H_{B_i} = \sum_{\mathbf{k}} \nu_{i,\mathbf{k}} b_{i,\mathbf{k}}^\dagger b_{i,\mathbf{k}}, \quad (9)$$

where the bosonic mode operators satisfy canonical commutation relations  $[b_{i,\mathbf{k}}, b_{j,\mathbf{k}'}^\dagger] = \delta_{ij} \delta_{\mathbf{k}\mathbf{k}'}$  and  $[b_{i,\mathbf{k}}, b_{j,\mathbf{k}'}] = 0$ . The qubit-bath interaction is given by

$$H_{AB} = \sum_{i=1}^3 A_i \otimes X_i \quad (10)$$

where  $A_i = \sigma_i^x$  and the collective bath coordinates are defined by

$$X_i = \sum_{\mathbf{k}} \left( \lambda_{i,\mathbf{k}} b_{i,\mathbf{k}} + \lambda_{i,\mathbf{k}}^* b_{i,\mathbf{k}}^\dagger \right), \quad (11)$$

with constants  $\lambda_{i,\mathbf{k}}$  that control the strength of the coupling of qubit  $i$  to its associated bath.

When  $g = 0$ , the eigenstates of the qubit Hamiltonian are simply the computational basis states. When  $g \neq 0$ , the interaction splits the degenerate states spanning the transport subspace into two new eigenstates, denoted by  $|\pm\rangle = (|101\rangle \pm |010\rangle)/\sqrt{2}$ , with corresponding energy eigenvalues  $E_2 \pm g$ . The remaining eigenstates and eigenvalues are left unchanged. The strong-coupling master equation describes dissipation as resulting from incoherent transitions between the eigenstates of the full coupled Hamiltonian  $H_A = H_{\text{loc}} + H_{\text{int}}$ .

We now sketch the derivation of the strong-coupling master equation, valid when  $g \gtrsim E_i$ . Working in an interaction picture with respect to  $H_A + H_B$ , the time evolution of the system coupling operators is given by

$$A_i(t) = e^{iH_A t} A_i e^{-iH_A t}.$$

We decompose this into Fourier components as

$$A_i(t) = \sum_{\omega} e^{-i\omega t} A_i(\omega), \quad [H_A, A_i(\omega)] = -\omega A_i(\omega), \quad (12)$$

where the  $\{\omega\}$  denote the set of all possible (positive and negative) energy differences between the eigenvalues of  $H_A$ .

We assume that the initial state of the system factorises as  $\rho(0) = \rho_A(0) \otimes_{i=1}^3 \rho_{B_i}$ , where  $\rho_{B_i} = \frac{1}{Z_i} e^{-\beta_i H_{B_i}}$ , and that the system-bath coupling is sufficiently weak that perturbation theory can be ap-

plied. The master equation is derived by projecting the interaction-picture von Neumann equation for the density operator onto the subspace spanned by states of the form  $\rho_A \otimes \rho_B$  and truncating the resulting equation at second order in the system-bath coupling (Born approximation). The Markov approximation then consists of assuming that the memory time of the bath is much shorter than all typical time scales of the reduced qubit evolution, see Ref. [25] for details. Tracing over the baths results in the following equation of motion for the qubit density operator  $\tilde{\rho}_A$  in the interaction picture:

$$\frac{d\tilde{\rho}_A}{dt} = \sum_{\omega, \omega'} \sum_{i=1}^3 e^{i(\omega' - \omega)t} \Gamma_i(\omega) \left[ A_i(\omega) \tilde{\rho}_A(t) A_i^\dagger(\omega') - A_i^\dagger(\omega') A_i(\omega) \tilde{\rho}_A(t) \right] + \text{h.c.}, \quad (13)$$

where we defined the self-energy

$$\Gamma_i(\omega) = \int_0^\infty dt e^{i\omega t} \langle X_i^\dagger(t) X_i(0) \rangle, \quad (14)$$

with  $X_i(t) = e^{-iH_{B_i}t} X_i e^{iH_{B_i}t}$ . In general, the self-energy can be written  $\Gamma_i(\omega) = \frac{1}{2} \gamma_i(\omega) + iS_i(\omega)$  where the real part  $\gamma_i(\omega)$  corresponds to an incoherent transition rate, and the imaginary part  $S_i(\omega)$  corresponds to an energy shift which we assume to be negligibly small.

We now perform the rotating-wave approximation by averaging over the oscillating terms in Eq. (13), so that terms with  $\omega \neq \omega'$  drop out. This approximation is valid when the typical energy differences are much larger than the incoherent transition rates, i.e.  $\min\{E_i, g\} \gg \max\{\gamma_i(\omega)\}$ . Transforming back to the Schrödinger picture results in a Lindblad equation of the form

$$\frac{d\rho_A}{dt} = -i[H_A + H_{\text{int}}, \rho_A] + \sum_{i=1}^3 \sum_{\omega} \gamma_i(\omega) \mathcal{D}[A_i(\omega)](\rho_A), \quad (15)$$

where the dissipators are given by

$$\mathcal{D}[L](\rho) = L \rho L^\dagger - \frac{1}{2} \{L^\dagger L, \rho\} \quad (16)$$

for a general Lindblad operator  $L$ . Explicitly, the Lindblad operators are given by

$$\begin{aligned} A_1(E_1) &= |011\rangle \langle 111| + |000\rangle \langle 100| \\ A_1(E_1 + g) &= \frac{1}{\sqrt{2}} (|001\rangle \langle +| - |-\rangle \langle 110|) \\ A_1(E_1 - g) &= \frac{1}{\sqrt{2}} (|+\rangle \langle 110| + |001\rangle \langle -|) \end{aligned}$$

$$\begin{aligned}
A_2(E_2) &= |100\rangle\langle110| + |001\rangle\langle011| \\
A_2(E_2 + g) &= \frac{1}{\sqrt{2}}(|000\rangle\langle+| + |-\rangle\langle111|) \\
A_2(E_2 - g) &= \frac{1}{\sqrt{2}}(|+\rangle\langle111| - |000\rangle\langle-|) \\
A_3(E_3) &= |110\rangle\langle111| + |000\rangle\langle001| \\
A_3(E_3 + g) &= \frac{1}{\sqrt{2}}(|100\rangle\langle+| - |-\rangle\langle011|) \\
A_3(E_3 - g) &= \frac{1}{\sqrt{2}}(|+\rangle\langle011| + |100\rangle\langle-|),
\end{aligned}$$

while the remaining non-zero Lindblad operators, corresponding to the reverse processes, are found from  $A_i(-\omega) = A_i(\omega)^\dagger$ .

In order to actually evaluate the rates  $\gamma_i(\omega)$ , we introduce the spectral function of each bath:

$$J_i(\omega) = 2\pi \sum_{\mathbf{k}} |\lambda_{i,\mathbf{k}}|^2 \delta(\omega - \nu_{i,\mathbf{k}}). \quad (17)$$

In the limit of an infinite bath with a smooth density of states, the sum over the quantum numbers  $\mathbf{k}$  can be approximated by an integral, and  $J_i(\omega)$  becomes a continuous function. We assume that the baths have identical spectral functions of the Ohmic form

$$J_i(\omega) = \alpha \omega e^{-\omega/\Omega}, \quad (18)$$

where  $\alpha$  is a dimensionless coupling parameter and  $\Omega$  is a cut-off frequency of the system-bath interaction, which must be much larger than all other energy scales in order for the Markov approximation to hold. The incoherent rates are then given by

$$\gamma_i(\omega) = \begin{cases} J_i(\omega)[1 + n(\omega, \beta_i)] & (\omega > 0) \\ J_i(|\omega|)n(|\omega|, \beta_i) & (\omega < 0) \end{cases}, \quad (19)$$

where  $n(\omega, \beta) = (e^{\beta\omega} - 1)^{-1}$  denotes the Bose-Einstein distribution.

### Weak-Coupling Master Equation

We now consider the case of Markovian dissipation with small  $g$ , with the same Hamiltonians describing the baths (9) and qubit-bath interactions (10). When the coupling  $g$  is comparable to the dissipation rates, the previous derivation is no longer valid since the rotating-wave approximation does not apply to counter-rotating terms of frequency  $(\omega - \omega') \sim g$ . In this case, we should work in an interaction picture generated by  $H_{\text{loc}} + H_B$  and treat the interaction  $H_{\text{int}}$  between the qubits as a small perturbation [18, 19]. The time evolution of the

system coupling operators is now given by

$$A_i(t) = e^{iH_{\text{loc}}t} A_i e^{-iH_{\text{loc}}t},$$

with the corresponding Fourier decomposition

$$A_i(t) = \sum_{\omega} e^{-i\omega t} A_i(\omega), \quad [H_{\text{loc}}, A_i(\omega)] = -\omega A_i(\omega),$$

where the frequencies  $\{\omega\}$  represent the eigenvalue differences of  $H_{\text{loc}}$  only.

As before, we assume that the initial state of the system factorises as  $\rho(0) = \rho_A(0) \otimes \rho_B$ . Now we project the interaction-picture von Neumann equation onto states of the form  $\rho_A \otimes \rho_B$  and truncate the resulting equation at second order in the qubit-bath interaction *and* the qubit-qubit interaction. We then perform the Markov approximation and trace over the bath variables; see Ref. [19] for full details of the derivation. The resulting equation of motion is

$$\begin{aligned}
\frac{d\tilde{\rho}_A}{dt} &= -i[H_{\text{int}}, \tilde{\rho}_A] \\
&+ \left( \sum_{\omega, \omega'} \sum_{i=1}^3 e^{i(\omega' - \omega)t} \Gamma_i(\omega) \left[ A_i(\omega) \tilde{\rho}_A(t) A_i^\dagger(\omega') \right. \right. \\
&\quad \left. \left. - A_i^\dagger(\omega') A_i(\omega) \tilde{\rho}_A(t) \right] + \text{h.c.} \right), \quad (20)
\end{aligned}$$

where the self-energy  $\Gamma_i(\omega)$  is defined by Eq. (14). We then write  $\Gamma_i(\omega) \approx \frac{1}{2}\gamma_i(\omega)$ , neglecting the imaginary part corresponding to small energy shifts of the qubit energy splittings. The rotating-wave approximation now consists of crossing off counter-rotating terms with  $\omega \neq \omega'$ , all of which have frequencies of order  $E_i$ . In order to be consistent with our assumptions, we must have  $E_i \gg g$ . The resulting master equation in the Schrödinger picture is

$$\begin{aligned}
\frac{d\rho_A}{dt} &= -i[H_A + H_{\text{int}}, \rho_A] \\
&+ \sum_{i=1}^3 [\gamma_i(E_i) \mathcal{D}[\sigma_i^-](\rho_A) + \gamma_i(-E_i) \mathcal{D}[\sigma_i^+](\rho_A)],
\end{aligned} \quad (21)$$

where the rates are given by Eq. (19).

### Fictitious Qubit Environment

In order to model non-Markovian environments, we introduce three additional fictitious qubits described by Pauli operators  $\tau_i^{x,y,z}$ , with Hamiltonian

$$H_F = \frac{1}{2} \sum_{i=1}^3 E_i \tau_i^z. \quad (22)$$

We have chosen these qubits to have identical energy splittings to their associated physical qubits, in order to avoid renormalising the physical qubit energy splittings. The coupling to the refrigerator is described by the Hamiltonian

$$H_{AF} = \sum_{i=1}^3 \lambda (\sigma_i^+ \tau_i^- + \sigma_i^- \tau_i^+), \quad (23)$$

where  $\sigma_i^\pm = \frac{1}{2}(\sigma_i^x \pm i\sigma_i^y)$  and  $\tau_i^\pm = \frac{1}{2}(\tau_i^x \pm i\tau_i^y)$ . We also introduce a Lindblad dissipator for each fictitious qubit corresponding to damping by a perfectly Markovian (delta-correlated in time) reservoir at temperature  $T_i$ . For simplicity, we assume identical spontaneous emission rates  $\gamma$  for the three fictitious qubits. The density operator  $\rho_{AF}$  of the six-qubit system is therefore described by the master equation

$$\begin{aligned} \frac{d\rho_{AF}}{dt} = & -i[H_A + H_F + H_{AF}, \rho_{AF}] \\ & + \gamma \sum_{i=1}^3 [\mathcal{D}[\tau_i^-](\rho_{AF}) + e^{-\beta_i E_i} \mathcal{D}[\tau_i^+](\rho_{AF})]. \end{aligned} \quad (24)$$

The effective spectral density seen by each physical qubit is of the Lorentzian form

$$J_i(\omega) = \frac{\lambda^2 \Gamma_i}{\Gamma_i^2 + (E_i - \omega)^2}, \quad (25)$$

where  $\Gamma = \gamma(1 + e^{-\beta_i E_i})/2$ . For a fixed  $\lambda$  and  $T_i$ , the bandwidth of the effective bath's frequency response is therefore controlled by modifying the parameter  $\gamma$ .

### Stochastic Absorption Refrigerator

For the stochastic absorption refrigerator, we set  $g = 0$  so that there is no Hamiltonian qubit-qubit coupling. Instead, the exchange of energy between the qubits is effected by the Lindblad operators  $B = |101\rangle\langle 010|$  and its adjoint  $B^\dagger$ . The thermalising effect of the baths is modelled using the same dissipators as the weak-coupling master equation (21). The total master equation therefore reads as

$$\begin{aligned} \frac{d\rho_A}{dt} = & -i[H_A, \rho_A] + \Gamma \mathcal{D}[B](\rho_A) + \Gamma \mathcal{D}[B^\dagger](\rho_A) \\ & + \sum_{i=1}^3 [\gamma_i(E_i) \mathcal{D}[\sigma_i^-](\rho_A) + \gamma_i(-E_i) \mathcal{D}[\sigma_i^+](\rho_A)], \end{aligned} \quad (26)$$

with rates given by Eq. (19). It is straightforward to demonstrate that the stochastic transport model is still energy-preserving, in the sense that  $\text{Tr} \{ H_{\text{loc}} \mathcal{D}[B](\rho_A) \} + \text{Tr} \{ H_{\text{loc}} \mathcal{D}[B^\dagger](\rho_A) \} = 0$ .